

Comparison of the paramagnetic spin fluctuations in nickel with asymptotic renormalization-group theory

P. Böni*

*Labor für Neutronenstreuung Eidgenössische Technische Hochschule and Paul Scherrer Institut,
CH-5232 Villigen PSI, Switzerland*

H. A. Mook

Solid State Division, Oak Ridge National Laboratory, Oak Ridge, Tennessee 37830

J. L. Martínez*

Instituto de Ciencia de Materiales, Universidad Autonoma de Madrid, E-28034 Madrid, Spain

G. Shirane

Brookhaven National Laboratory, Upton, New York 11973

(Received 26 May 1992)

The paramagnetic spin fluctuations in Ni have been investigated at small momentum \mathbf{q} and energy transfer $\hbar\omega$ by means of inelastic-neutron-scattering techniques. For fixed energy transferred from the neutron to the spin system [$S(q, \omega = \text{const})$], peaks at finite momentum are observed. Their positions are very sensitive to the low-intensity parts of the magnetic cross section. The results are compared with an analytical expression for the dynamical correlation function for an isotropic ferromagnet introduced by Iro. The agreement with the theory is good near T_c for excitation energies $1 \text{ meV} \leq \hbar\omega < k_B T_c \simeq 50 \text{ meV}$. Further away from T_c serious discrepancies occur, mainly because the spin fluctuations slow down more quickly than expected on the basis of mode-mode coupling or renormalization-group theory. If the experimentally determined scaling function is used, then the results can be well parametrized. The additional slowing down, which affects also the line shape at T_c , is most likely caused by the interaction of the $3d$ moments with the conduction electrons, i.e., by an itinerant effect. We have also extracted from our data the asymptotic behavior of the scattering function at very large energy transfers, i.e., $S_I(q, \omega \rightarrow \infty) \propto \omega^{-(z+4)/2}$ at T_c and the results are in reasonable agreement with renormalization-group theory. No indications for a breakdown of dynamical scaling has been found within the q and E ranges investigated.

I. INTRODUCTION

The properties of several isotropic ferromagnets have been investigated extensively during the past few years, in order to characterize the interplay between itinerant and local moments above T_c . The underlying physics is well understood in the limit of localized moments in terms of exchange interactions and in the opposite limit in terms of the theory of weak itinerant magnetism.¹ The magnetic order vanishes in the former case because the magnetic moments (with fixed amplitude) disorder due to thermal excitations via spin waves, whereas in the latter case the exchange splitting decreases. Although the spin dynamics of the well-known $3d$ ferromagnets Fe and Ni resemble qualitatively those of localized magnets, like EuO and EuS at small q , it became apparent that the magnetic properties close to or above T_c cannot be described by means of either of the two theories mentioned above. In contrast, the low-temperature behavior of the spin dynamics in $3d$ metals can only be understood on the basis of band theory. Mook and collaborators have determined the spin-wave dispersion curve in Ni (Ref. 2) and

Fe (Ref. 3) mostly at room temperature up to 200 meV and found reasonably good agreement with band calculations performed by Cooke, Blackman, and Morgan for $T=0 \text{ K}$ in Ni.⁴ Unfortunately, band calculations cannot be simply extended to finite temperatures because the feedback of the spin fluctuations on the band structure is difficult to accomplish.

In 1973 Mook, Lynn, and Nicklow⁵ measured the differential neutron-scattering cross section in paramagnetic Ni and discovered well-defined peaks at finite momentum transfer q_0 when the energy transfer ($\hbar\omega > 12 \text{ meV}$) from the neutron to the spin system was kept fixed (constant- E scans). These peaks seemed to define a dispersion-like curve (Fig. 1). Further investigation of the paramagnetic scattering revealed, however, that constant- E peaks are a general property of isotropic ferromagnets⁶ and that their location q_0 is well reproduced by $\hbar\omega_0 = 1.27 A q_0^z$, $z = 2.5$, $A = 350 \text{ meV \AA}^{2.5}$, independent of the degree of localization of the magnetic moments.⁷

The observation of constant- E peaks in the paramagnetic phase was at first rather puzzling because the widely used scattering function

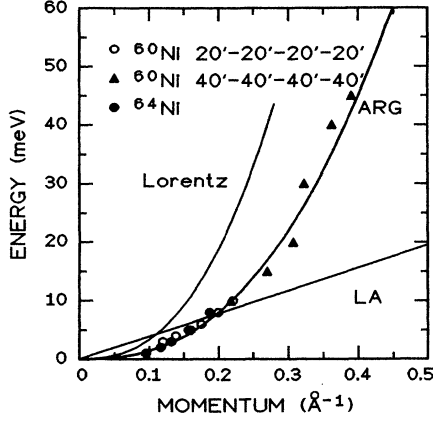


FIG. 1. Constant- E scan peak positions in Ni at T_c . The bold solid line is the prediction of asymptotic renormalization-group theory (ARG). The thin solid line is the calculation based on a Lorentzian spectral weight function. The dispersion curve for the longitudinal acoustic (LA) phonon is also shown.

$$S(q, \omega) = 2k_B T \chi(0) \frac{\kappa^2}{\kappa^2 + q^2} F(q, \omega) \frac{\hbar\omega/k_B T}{1 - \exp(-\hbar\omega/k_B T)} \quad (1)$$

with

$$F(q, \omega) = F_L(q, \omega) = \frac{1}{\pi} \frac{\Gamma}{\Gamma^2 + \hbar\omega^2} \quad (2)$$

yields at T_c for the peak position $\hbar\omega_0 = 3\Gamma$ (see Fig. 1). $\chi(0)$ is the static susceptibility, κ the inverse correlation length ($\kappa = 0$ at T_c), and the other symbols retain their usual meaning. The linewidth is given by $\Gamma = A f(\kappa/q) q^{2.5}$, where the dynamical scaling function $f(\kappa/q)$ has been calculated by Résibois and Piette⁸ on the basis of mode-mode coupling theory. The observed discrepancy between prediction and experiment was shown to be caused by the non-Lorentzian shape of the spectral shape function.⁹

In 1985 Folk and Iro¹⁰ introduced a spectral shape function $F_c(q, \omega)$ at $T = T_c$, which is based on the renormalization-group approach by Dohm¹¹ for an isotropic ferromagnet at T_c in $6 - \epsilon$ dimensions and on an interpolation formula by Bhattacharjee and Ferrell:¹²

$$F_c(q, \omega) = \frac{1}{\pi} \frac{1}{A q^{2.5}} \text{Re} \frac{1}{is + \alpha [1 + i(a/\alpha)s]^{-0.6}}, \quad (3)$$

where $\alpha = 0.78$, $a = 0.46$, and $s = \omega/\omega_c$. The characteristic energy ω_c for a Lorentzian spectral weight function [Eq. (2)] is equal to Γ . They demonstrated that F_c describes well the available data of Fe and Ni at T_c . More recent experiments in the localized systems EuO (Ref. 13) and EuS (Ref. 14) also confirmed the validity of asymptotic renormalization-group theory at T_c . The extension of this theory to $T > T_c$ predicts that (i) the position q_0 is almost independent of T and (ii) the width δq of the

constant- E peaks increases with T .¹⁵ Such a behavior is born out qualitatively by the original data of Mook, Lynn, and Nicklow.⁵ Although $F_c(q, \omega)$ was only known in the limits $T = T_c$ and $T = \infty$, dynamical scaling predicts that the scaled position $q_0^* = q_0(A/\hbar\omega)^{0.4}$ and the scaled width $\delta q^* = \delta q_0(A/\hbar\omega)^{0.4}$ lie on universal curves, respectively, when plotted versus $\log_{10}(\hbar\omega/A\kappa^{2.5})$.

Recently Iro calculated the dynamic correlation function for an isotropic ferromagnet in first order in $\epsilon = 6 - d$ for $T > T_c$,¹⁶ verifying the original results.¹⁵ However, the expression thus obtained turns out to be too complicated for a direct comparison with experimental data. Therefore, Iro proposed an analytical expression for the scattering function, which is more suitable for comparison,¹⁷ namely,

$$F_I(q, \omega, \kappa) = \frac{1}{\pi\omega_c} \text{Re} \frac{1}{-is + \frac{1}{Z(x)\Pi_1(x, iW)}}, \quad (4)$$

$$x = q/\kappa,$$

where the self-energy Π_1 of the dynamic susceptibility is

$$\Pi_1(x, iW) = \left[\left[1 + \frac{b}{x^2} \right]^{2-\epsilon/4} - aiW \right]^{\epsilon/(8-\epsilon)} \quad (5)$$

with $a = 0.46$ (as above), $b = 3.16$, and $\epsilon = 6 - d = 3$. This choice of Π_1 indeed reproduces the correct asymptotic behavior

$$F_I(q, \omega \rightarrow \infty, 0) \propto \omega^{-(z+4)/z} = \omega^{-2.6} \simeq \omega^{-(2+\epsilon/8)}$$

at T_c as predicted by renormalization-group theory.¹¹ $Z(x)$ is given by ($k = 0.51$)

$$Z(x) = \left[1 - k \arctan \left[a \frac{1 + 1/x^2}{(1 + b/x^2)^2} \right] \right]^{-1} \times \left[1 + \frac{b}{x^2} \right]^{-\epsilon/4}. \quad (6)$$

$Z(x)$ is closely related to the dynamical scaling function Ω via

$$\Omega(x) = \frac{Z(x)}{X(x)Z(\infty)}. \quad (7)$$

$\Omega(x)$ agrees with the Résibois-Piette function $f(\kappa/q)$ within 10%. $X(x) = (1 + 1/x^2)^{-1}$ is the static scaling function, and $W = \hbar\omega Z(\infty)/(Aq^{2.5})$ is a scaled energy at the critical point. Note that the constant α from Eq. (3) is equal to $1/Z(\infty)$. Actually $F_I(q, \omega, x = \infty)$ is identical to $F_c(q, \omega)$ [Eq. (3)] and $F_I(q, \omega, x = 0)$ is identical to $F_L(q, \omega)$ [Eq. (2)].

In order to test the proposed spectral weight function given by Eq. (3) and the underlying physics we performed neutron-scattering measurements at small q in the paramagnetic phase of Ni in the range $1 \leq \hbar\omega \leq 45$ meV and for temperatures $T_c \leq T \leq 1.48T_c$ ($T_c = 631$ K). We have chosen Ni for this experiment because a large energy range can be covered using normal triple-axis spectroscopy (in contrast to EuS or EuO), and because the dipolar interactions in Ni are very weak¹⁸ and can be

neglected. Moreover, we hoped to find indications for itinerant effects. A short account of the present work has been given elsewhere.¹⁹

II. EXPERIMENT

The neutron-scattering experiments were conducted on the triple-axis spectrometers *H4m* and *H7* at the High Flux Beam Reactor at Brookhaven National Laboratory. Pyrolytic graphite crystals set for the (002) reflection were used for the monochromator and the analyzer. The final neutron energy E_f was kept fixed at 14.7 meV and the collimations were all 20' or 40' depending upon the conflicting requirements of resolution and reasonable intensity. Higher-order neutrons were removed by means of a pyrolytic graphite filter. The counting time for all data has been normalized to a constant number of neutrons incident on the sample.

For our experiments we have used two samples: a large (403 g) isotopically enriched single crystal ^{60}Ni grown at Oak Ridge National Laboratory, which proved to be very useful at large energy transfers and a small (16 g) isotopically enriched single crystal ^{64}Ni grown at Brookhaven National Laboratory. The latter sample proved to be particularly useful for the measurements at small energy transfers because the nuclear scattering length of ^{64}Ni is almost zero. Hence, there are neither nuclear Bragg peaks nor phonons that disturb the measurements. The lattice constant of Ni is 3.53 Å yielding a nearest inverse plane distance $d_{111} = 3.09 \text{ \AA}^{-1}$.

The samples were mounted with the [111] axis horizontal inside an evacuated furnace of spherical shape. The Curie temperature $T_c = 631 \text{ K}$ was determined by measuring the critical scattering at small q . The uncertainties are as follows: $T_c \pm 2 \text{ K}$ for ^{60}Ni and $T_c \pm 5 \text{ K}$ for ^{64}Ni . The measurements were conducted near the (111) Bragg reflection in the [111] direction. The temperature control was stable to within $\pm 0.5 \text{ K}$ over the period of our measurements.

III. RESULTS

The paramagnetic scattering data has been measured using constant momentum and constant energy scans. First we show the temperature dependence of some constant- q scans, which yield direct information about the lifetime of the paramagnetic fluctuations and explain how the nonmagnetic scattering was removed from the data. Then we present constant- E scans, which contain information on the line shape of the magnetic cross section and on the dynamics. Finally we show that the two data sets can be parametrized in a consistent fashion on the basis of the expression derived by Iro from asymptotic renormalization-group theory.

A. Results from constant- Q scans

Constant- Q scans were conducted at $(1+\zeta, 1+\zeta, 1+\zeta)$ ($\zeta=0.03$ or 0.04) and five different temperatures using the large ^{60}Ni sample. Figure 2 shows the result for $\zeta=0.04$. We have subtracted from the data an energy independent background of 2 counts/min and the scatter-

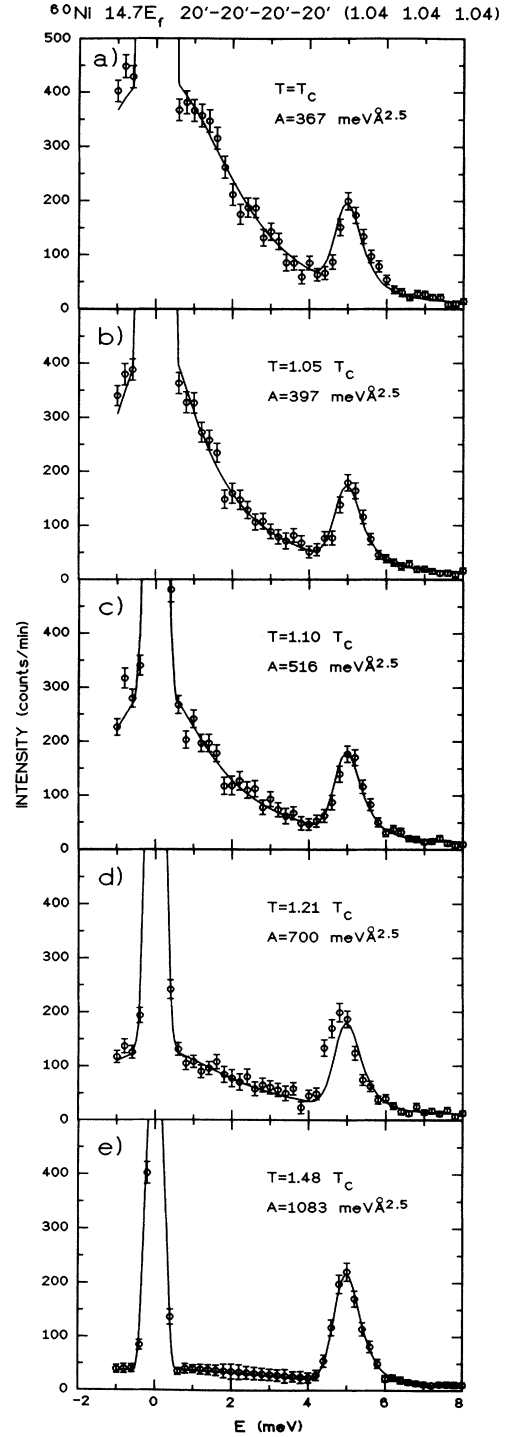


FIG. 2. T dependence of constant- Q scans at $\zeta=0.04$ ($q=0.012 \text{ \AA}^{-1}$). A constant background of 2 counts/min and the intensity from the transverse acoustic (TA) phonon has been subtracted. The solid lines through the data are fits using the cross section based on asymptotic renormalization-group theory.

ing from the transverse-acoustic phonon that appears between 2 and 3.5 meV (as explained below). The spectra still contain a large elastic peak due to incoherent scattering, mostly from the sample, and the well-defined longitudinal phonon near 5 meV. The broad peak of magnetic scattering decreases rapidly with increasing temperature and the width decreases first and then increases again. The solid lines through the data are fits, using F_I [Eq. (4)] as a spectral weight function in the expression for the scattering function. The fits reproduce the data reasonably well. The fit parameters were an amplitude N for the paramagnetic scattering, the spin diffusion constant A , and amplitudes P and B for the LA phonon and the incoherent scattering, respectively. It is gratifying that the spin diffusion constant at T_c , $A = 367 \pm 18 \text{ meV } \text{Å}^{2.5}$, is within the accepted experimental value $A = 350 \text{ meV } \text{Å}^{2.5}$.²⁰

On the basis of Fig. 3 we explain how the scattering from the transverse-acoustic (TA) phonons was removed from the raw data. In principle, the shape of the TA phonons can be calculated as shown by Skalyo and Lurie²¹ because the vertical collimation of the spectrometer is known. However, we found it more convenient to subtract the TA phonon directly from the measurements because its intensity is small and the resulting corrected spectra are easier to understand.

In order to extract the intensity of the TA phonon we have convoluted $S(q, \omega)$ with the resolution function of the spectrometer. The thin solid line in Fig. 3 is a fit to the data ($T = 1.48T_c$) with the amplitudes for the incoherent scattering B and the LA phonon P as fitting parameters. The velocity of sound for Ni is known and was fixed at $39.1 \text{ meV } \text{Å}$. The parameters for the magnetic scattering were chosen as follows: $A = 350 \text{ meV } \text{Å}^{2.5}$ and $\kappa = \kappa_0 t^{0.702}$ [$t = (T - T_c)/T_c$], where $\kappa_0 = 0.7874 \text{ Å}^{-1.22}$. The normalization constant N was fixed at a value that was obtained by fitting the paramagnetic scattering near T_c , where the intensity of the TA phonon is small compared with the paramagnetic scattering [Fig. 2(a)]. The data are obviously incompatible with the fit because the

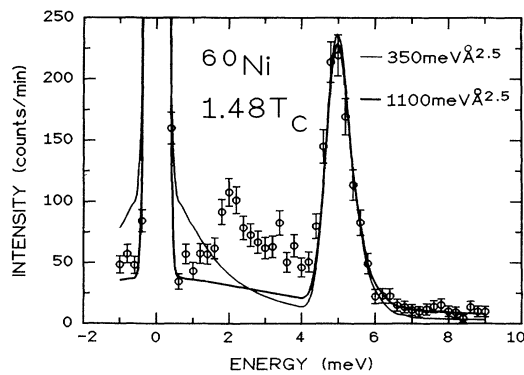


FIG. 3. Constant- Q scan measured at $1.48T_c$. A constant background of 2 counts/min has been subtracted. The integrated intensity of the fitted paramagnetic scattering was fixed. Thin solid line: calculation with $A = 350 \text{ meV } \text{Å}^{2.5}$; bold solid line: calculation with $A = 1100 \text{ meV } \text{Å}^{2.5}$.

width of the magnetic scattering is too small: the neutron intensity near 1 meV is overestimated and the intensity near 7 meV is underestimated by the fit. Therefore, we adjusted A for fixed N in such a way that these discrepancies were minimized. The bold solid line in Fig. 3 shows that $F_I(q, \omega, \kappa)$ with $A = 1100 \text{ meV } \text{Å}^{2.5}$ reproduces the data rather well indicating that $\Omega(x)$ [Eq. (7)] does not agree with the measured dynamical scaling function of Ni. The difference intensity $\Delta I = I_{\text{obs}} - I_{\text{fit}}$ between 1 and 4 meV was assumed to be the contamination by the TA phonon and hence subtracted from all scans at $\zeta = 0.04$ (see Fig. 2). An identical procedure was adopted for the scans at $\zeta = 0.03$.

These corrections ($\Delta I < 75 \text{ c/min}$) are safe for $T \leq 1.21T_c$ because the magnetic scattering is strong. An indication for the self-consistency of the corrections is the fact that the fitted value $A(T = 1.48T_c) = 1083 \pm 132 \text{ meV } \text{Å}^{2.5}$ [see Fig. 2(e)] is very close to the assumed value of $1100 \text{ meV } \text{Å}^{2.5}$. The T dependence of the normalization constant for the magnetic scattering, N , and the spin diffusion constant, A , is also reproduced well, indicating that the corrections are done consistently. In addition, the phonon intensities are correct too.

From the knowledge of the linewidths at different temperatures the dynamical scaling function $\Omega(x) = \Gamma(T)/\Gamma(T_c)$ can be determined. Figure 4 shows that $\Omega(x)$ for Ni as obtained in this study is compatible with earlier data²³ within the range $0 < 1/x < 1$, however, it clearly disagrees for $1/x > 1$ with the predictions of mode-mode coupling theory and asymptotic renormalization-group theory. At high T (small x) the broadening is about three times larger.

In order to parametrize the measured dynamical scaling function we have used the expression from Iro, Eq. (7), as a heuristic model and have treated the parameters a , b , and k as fit parameters, obtaining -70 , 3.2 , and 1.5 , respectively. We emphasize that these new parameters also invoke a change of the shape of the spectral weight

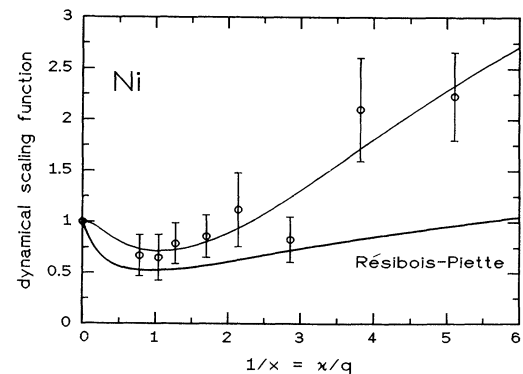


FIG. 4. Dynamical scaling function (circles) as deduced from constant- Q scans. The error bars represent statistical errors only. For large $1/x = \kappa/q$ ($T \gg T_c$) the deviations from the mode-mode coupling result (bold solid line) (Ref. 8) are significant. The thin solid line is a parametrization of the data as explained in the text.

function at and near T_c , however, not in the limit $T \rightarrow \infty$, where F_T is still a simple Lorentzian [Eq. (2)].

B. Results from constant- E scans

Constant- E scans were performed at eight different temperatures $T_c \leq T \leq 1.48T_c$ for energy transfers $1 \leq \hbar\omega \leq 45$ meV. In Fig. 5, we show the T dependence of the scattering for $\hbar\omega = 1$ meV as measured in ^{64}Ni . Near T_c the peak is well defined. Its intensity decreases and broadens with increasing T . Initially, the peak position does not change much as expected on the basis of the work by Folk and Iro.⁵ However, at $1.19T_c$ the peak shifts to smaller q . The scans at 1 meV are most interesting with regard to the present work, because the scaling variable $x = q/\kappa$ changes most dramatically in a constant- E scan. In Fig. 6, the E dependence of the paramagnetic scattering at T_c is compared with the asymptotic renormalization-group theory prediction (solid line, $A = 350 \text{ meV \AA}^{2.5}$). The agreement with theory is good over the impressive E range $1 \leq \hbar\omega \leq 30$ meV. We emphasize that the measured cross sections are very small because the magnetic scattering is only measured in the tails of the cross section where the intensity

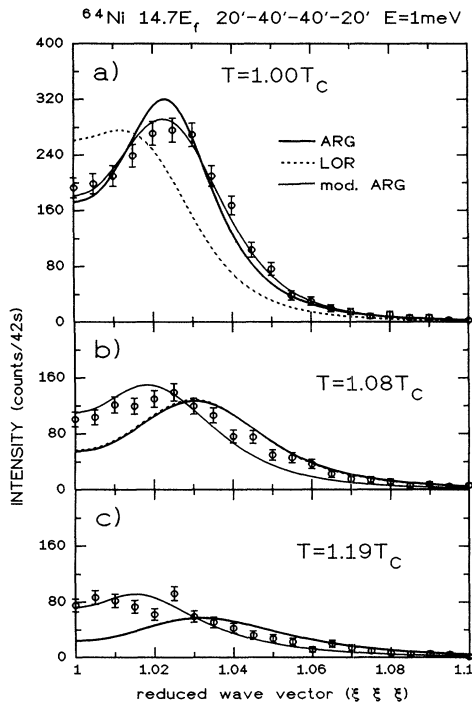


FIG. 5. T dependence of constant- E scans for $\hbar\omega = 1$ meV conducted in ^{64}Ni . Also shown are the predictions of asymptotic renormalization-group theory (bold solid line), the modified cross section (thin solid line), and the cross section using a Lorentzian spectral weight function (dotted line). The spin diffusion constant was fixed at $A = 350 \text{ meV \AA}^{2.5}$. A background of 2 counts/42s has been subtracted. At high temperature the asymptotic renormalization-group theory cross section is equivalent to the Lorentzian approximation.

of the quasielastic scattering is small. The spectral weight has its maximum always at $\omega = 0$ (Fig. 2).

There are, however, significant deviations near $q = 0$, namely, the intensities from both samples are always roughly a factor of 2 larger than predicted, indicating that the spectral weight function as calculated with asymptotic renormalization-group theory is indeed only an approximation as stated by Folk and Iro in their original paper¹⁰ because the expansion parameter $\epsilon = 3$ is large. Looking back to similar measurements in Ni,²⁴ EuO,¹³ and EuS,¹⁴ there are also subtle indications for such discrepancies; however, they were at the border of

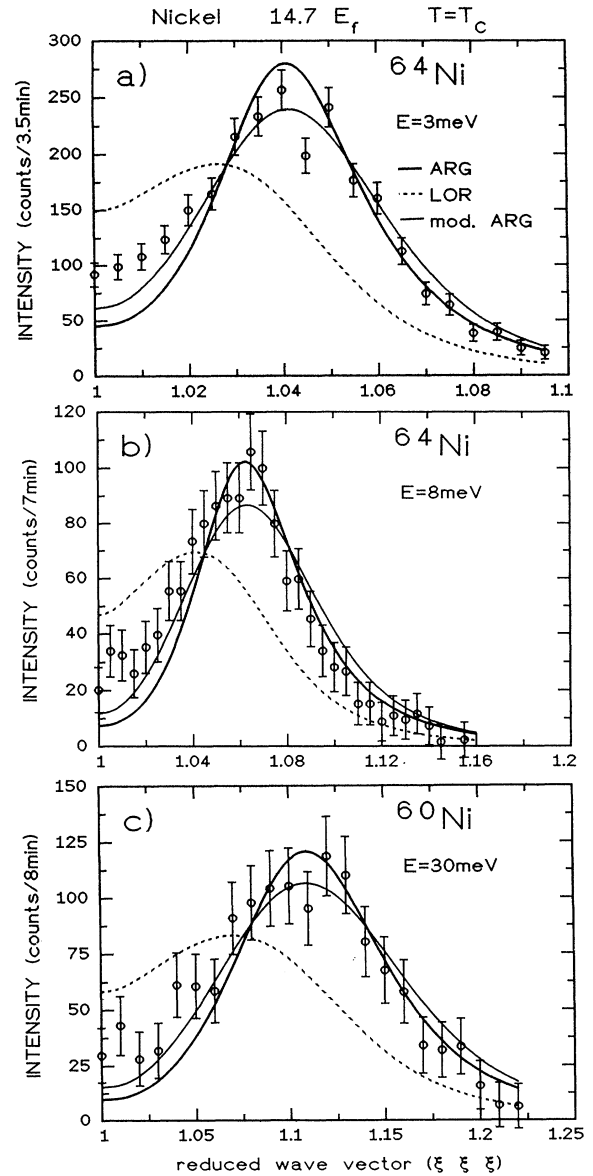


FIG. 6. Selection of constant- E scans in Ni at T_c . The scan at $\hbar\omega = 30$ meV was measured with ^{60}Ni . The lines have the same meaning as in Fig. 5. A constant background of 7, 15, and 32 counts has been subtracted from the data at 3, 8, and 30 meV, respectively.

being significant.

Finally, we present in Figs. 7 and 8 the T dependence of constant- E peaks for an intermediate and a very large energy transfer, respectively. At 8 meV the peaks are de-

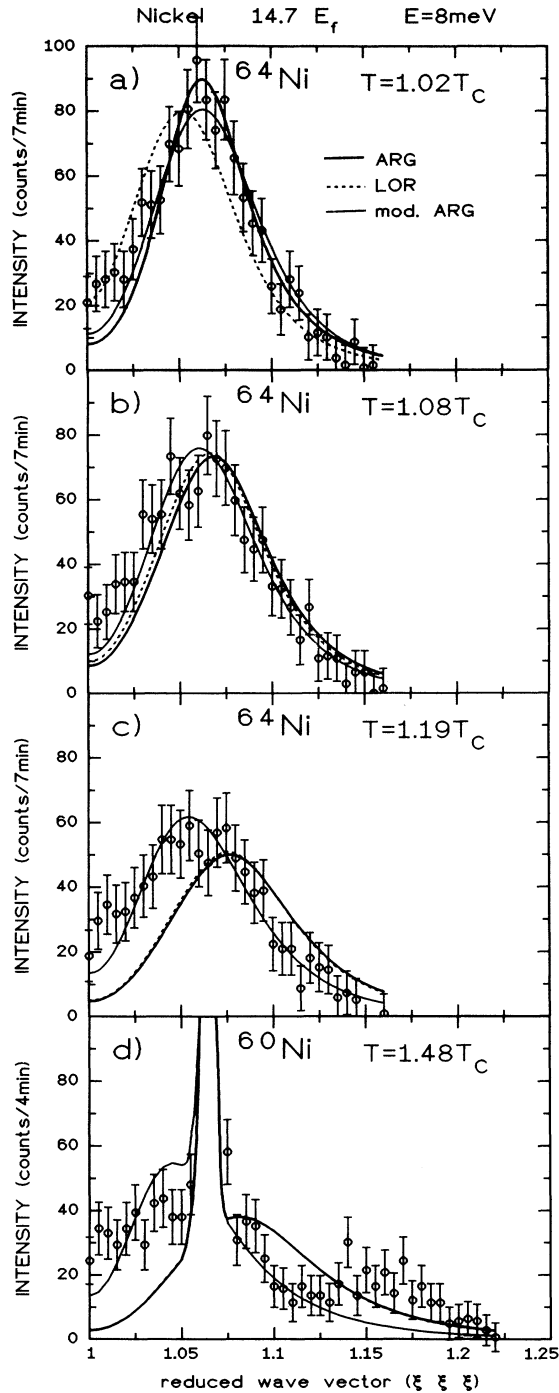


FIG. 7. T dependence of constant- E scans at $\hbar\omega=8$ meV. The scan at $1.48T_c$ was measured with the ^{60}Ni sample. The lines have the same meaning as in Fig. 5. Close to T_c the agreement with asymptotic renormalization-group theory is good.

creasing more quickly with increasing T than at 45 meV. This observation is an indication for the scaling behavior of the paramagnetic scattering, namely, increasing the temperature affects first the cross sections at small q and small ω . Note that the last scan in Fig. 7 was measured on ^{60}Ni . The LA phonon ($\hat{I}=366$ counts) is rather strong. The weak scattering near $\xi=1.16$ originates from the TA phonons due to the coarse vertical q resolution of the spectrometer.

At this point it might be interesting to compare the magnetic scattering intensities from the two samples. According to the constant- E scans at 8 meV we find that the counting time (7 min/point) for ^{64}Ni is roughly twice that for ^{60}Ni (4 min). However, the collimation for the former sample was more relaxed yielding four times more

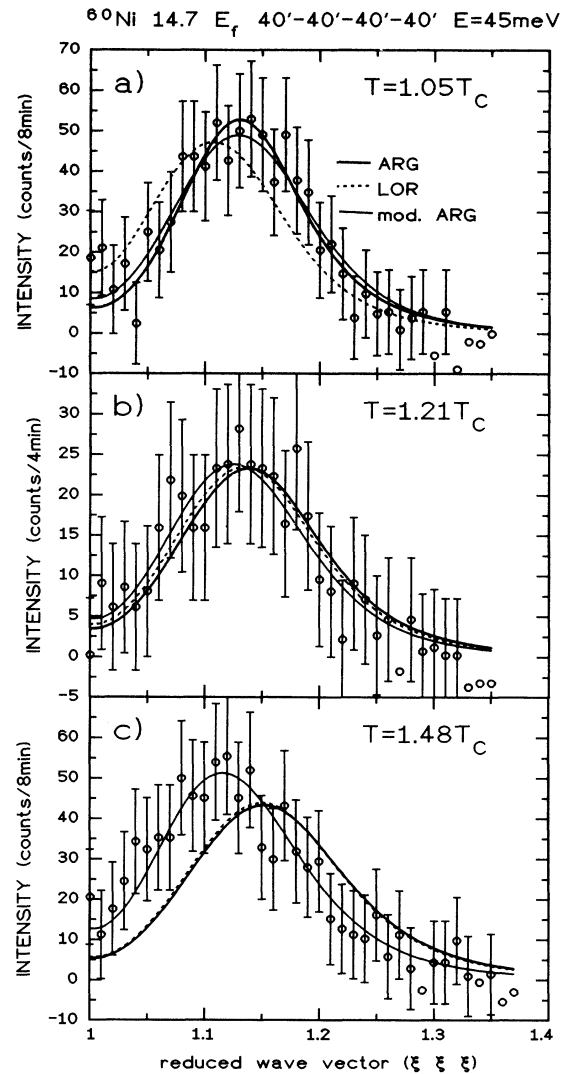


FIG. 8. T dependence of constant- E scans at large energy transfers $\hbar\omega=45$ meV. All scans have been measured with the ^{60}Ni sample. The lines have the same meaning as in Fig. 5. The agreement with asymptotic renormalization-group theory is good up to $1.21T_c$.

flux and $\approx 50\%$ coarser E resolution. Therefore, the counting time for ^{64}Ni is effectively ≈ 8 times longer than for the 25 times heavier ^{60}Ni sample with the same resolution conditions.

C. Parametrization of the data

Before comparing the T dependence of the magnetic scattering with the analytical expression proposed by Iro,¹⁷ we discuss in detail the magnetic cross section that we have used throughout this paper. It is given by

$$\frac{d^2\sigma}{d\Omega d\omega} = \gamma_0^2 \frac{k_f}{k_i} \left| \frac{1}{2} g F(\mathbf{Q}) \right|^2 e^{-2W} \times \sum_{\alpha, \beta} (\delta_{\alpha\beta} - \hat{Q}_\alpha \hat{Q}_\beta) S^{\alpha\beta}(\mathbf{Q}, \omega), \quad (8)$$

where $\gamma_0^2 = 0.291$ barns/sr, k_f and k_i are the wave vectors of the final and incident neutrons, g is the gyromagnetic ratio, $F(\mathbf{Q})$ is the form factor, and $\exp(-2W)$ is the Debye-Waller factor. $S^{\alpha\beta}$ is the spatial and temporal Fourier transform of the spin-spin correlation function for the Cartesian components α and β . The term $\delta_{\alpha\beta} - \hat{Q}_\alpha \hat{Q}_\beta$ selects those components of the scattering law that are perpendicular to the scattering vector \mathbf{Q} . In the isotropic case $\alpha = \beta$ and the sum over α and β reduces to $4/3 S(q, \omega)$, where $S(q, \omega)$ is given by Eq. (1).

We emphasize that the inclusion of the Debye-Waller factor is very important because the intensities are affected by this term by more than 20% over the q and T range of our measurements. The form factor was also always included in the fitting procedure. Both factors lead to a decrease of the magnetic intensity at large q . During the fitting procedure we have parametrized the product $k_B T \chi(0) \kappa^2$ by $NT^{2.4}$ [see also Eq. (1)]. The reasoning is as follows: Paramagnetic scattering from EuO and EuS indicates²⁵ that $\chi(0) \propto [T/(T - T_c)]^{1.4}$ and that $\kappa \propto [(T - T_c)/T_c]^{0.69}$ for $T_c < T < 1.5T_c$. Therefore $\chi(0) \kappa^2 \approx T^{1.4}$.

All the data in Figs. 2–8 have been fitted or compared with the above cross section (bold solid line). The results can be summarized as follows. The T dependence of the magnetic scattering agrees reasonably well with the predictions of asymptotic renormalization-group theory close to T_c , the range of application of the theory. The smaller the transferred energy, the lower is the temperature where discrepancies become significant, i.e., for 1 meV above $1.08 T_c$, for 8 meV above $1.1T_c$, and for 45 meV above $1.21T_c$. The cross sections, assuming a Lorentzian spectral weight function, are also shown (dashed lines). They reproduce the scattering well above T_c , however, significant deviations occur at T_c .

In Fig. 4, we have demonstrated that the experimentally determined scaling function of Ni deviates from the mode-mode coupling result. Obviously these discrepancies must also be reflected in constant- E scans. In order to make a fair comparison with the theory we have inserted into the cross section the measured $\Omega(x)$ via the fitted parameters a , b , and k , and compared the result with our measurements in Figs. 5–8 (thin lines). In fact, the agreement between measurement and the calculation

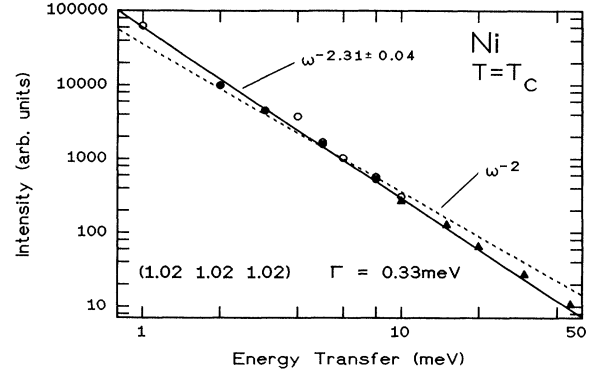


FIG. 9. Asymptotic behavior of the scattered intensity at (1.02 1.02 1.02) vs energy in a log-log representation. The half width at half maximum of the quasielastic scattering is 0.33 meV, i.e., more than 100 times smaller than the maximum energy probed in the experiment. The solid line indicates a fit to the data. The theoretical value for the exponent is ≈ -2.6 .

has now significantly improved.

Finally, we have constructed a constant- q scan using the constant- E data in order to investigate the asymptotic behavior of the spectral weight function at very large E transfers. Such data cannot be measured directly in one single constant- q scan because the intensity at large ω is orders of magnitude smaller than at $\omega = 0$. Figure 9 shows the asymptotic behavior for (1.02 1.02 1.02). The data points have been measured using three different spectrometer configurations and they have been normalized with each other near the overlapping region of 10 meV. The measurements can be well fitted by a power law $I(\omega) \propto \omega^{-p}$ with $p = 2.31 \pm 0.04$ over an impressive range of 4 decades in intensity. The exponent differs clearly from the value $p_L = 2$ expected for a Lorentzian. It is, however, smaller than expected from renormalization-group theory ($p = 2.6$), possibly because of the normalization procedure.

IV. DISCUSSION

The main purpose of the experiment was the comparison of the paramagnetic scattering from Ni with asymptotic renormalization-group theory. It predicts, in particular, a T -dependent spectral weight function, or, in other words, a change in the relaxational mechanisms responsible for the decay of the spin fluctuations, for which constant- E scans are most sensitive. Close to T_c , the agreement between theory and data is satisfactory with regard to the peak position in constant- E scans. However, the measured peak widths δq_0 are larger. At high T there are significant deviations from the theory even in the position q_0 . In order to compare our data with the theory in more detail we have plotted in Fig. 10 the scaled position $q_0^* = q_0 (A/\hbar\omega)^{0.4}$ and width $\delta q_0^* = \delta q_0 (A/\hbar\omega)^{0.4}$ versus the scaling variable $\tau^* = \log_{10}(\hbar\omega/A\kappa^{2.5})$ ($\tau^* \rightarrow \infty$ for $T \rightarrow T_c$), and compare them with the results of Ref. 17. First of all, the data ex-

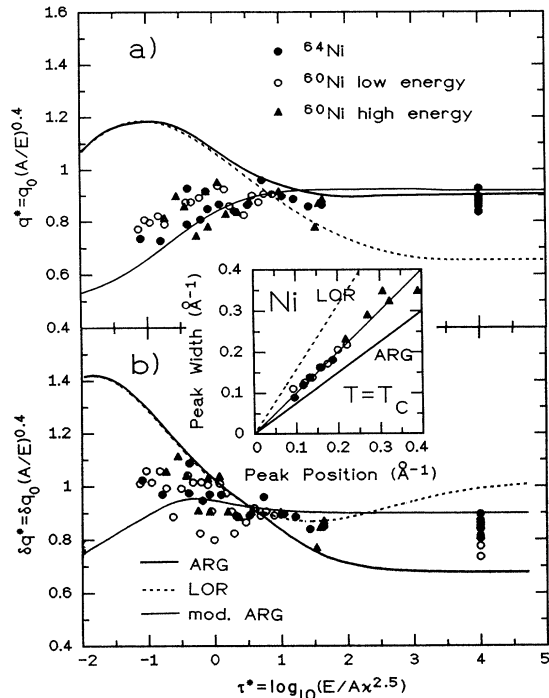


FIG. 10. Scaling plots for (a) position q_0^* and (b) width δq_0^* of constant- E peaks vs τ^* . The points at $\tau^*=4$ correspond to the measurements at T_c . The bold solid lines are the predictions of asymptotic renormalization-group theory, the thin solid lines are based on the parameterizations of the dynamical scaling function (Fig. 4) as explained in the text. The dotted lines correspond to the Lorentzian approximation for the spectral weight function. The inset shows δq vs q_0 as measured in constant- E scans at T_c .

hibit scaling behavior with respect to position and width over a large range in T and ω (note the logarithmic scale). Second, there are serious, systematic discrepancies for $\tau < 0$, i.e., at high T and small ω , as observed already in the raw data (Figs. 5, 7, and 8).

The use of the modified scaling function [Eq. (6)] with $a = -70$, $b = 3.2$, and $k = 1.5$ in the expression for the spectral weight function [Eq. (4)] improves the agreement between the measured and the calculated scaling behavior of q_0 and δq_0 . It is gratifying that the constant- Q and the constant- E data of both samples are now essentially compatible with each other. We emphasize that the modified scaling function not only affects the widths of the constant- E and constant- Q peaks above T_c , it also affects the line shape at all temperatures, in particular, the width of the constant- E peaks at T_c : namely, δq_0 is 25% [Fig. 10(b)] larger than the theoretical prediction, whereas the position is only slightly affected. In fact, the agreement of the peak shape with the data at T_c ($\tau^* = \infty$) has now significantly improved [see Fig. 5(a)]. Similar studies in EuO (Ref. 13) and EuS (Ref. 14) revealed that the experimental peak shapes of the (transverse) paramagnetic scattering at T_c agree well with asymptotic renormalization-group theory using the original parameters a , b , and k , indicating that there may be additional damping mechanisms in the paramagnetic phase of Ni

possibly due to the itinerancy of Ni.

At small τ^* deviations from the modified cross section become apparent, in particular, with regard to δq_0 [see Fig. 5(c)]. The most likely reasons to explain the discrepancies are that Ni is a $3d$ magnet, or the assumption that κ exhibits critical behavior over the wide T range investigated. However, the latter effect seems to be too small for explaining the serious discrepancies. Unfortunately, constant- E measurements in model Heisenberg systems extend only down to $\tau^* \simeq 1$ (Refs. 13 and 14) and definite conclusions about the applicability of asymptotic renormalization-group theory at smaller τ^* cannot be drawn.

For completeness we show in the inset of Fig. 10 peak position versus peak width as measured at T_c in this study and by Mook, Lynn, and Nicklow⁵ (see also Ref. 26). Such representations have been used in the past for discussing the validity of dynamical scaling²⁶ and for discussing crossover effects in line shapes.²⁷ Any scaling function yields a linear dependence $\delta q_0 = c q_0$, where c depends on the shape function. For a Lorentzian $c = 1.573$,²⁶ for a Gaussian $c = 0.552$,²⁷ and asymptotic renormalization-group theory yields $c = 0.75$.¹⁰ Our measurements show that within the q and E range investigated the concept of dynamical scaling is valid and there is no need to involve any crossover of the spectral weight function from a Lorentzian to another line shape as proposed recently,²⁷ although line-shape changes indeed occur at small q (Ref. 28) due to dipolar effects^{29,30} and at large q .^{31,32} However, we find a nontrivial deviation of c from the theoretical value, possibly related to itinerant effects to be discussed below.

The additional damping of the spin fluctuations is most likely caused by the interaction of the conduction electrons with the magnetic moments. An additional T -dependent and, at most, weakly q -dependent damping term can explain some of the discrepancies that we observe in our experiment: (i) The spin fluctuations are more damped at high T than in a localized magnet (Fig. 4), and (ii) the constant- E peaks shift to $q_0 = 0$ [Fig. 5(c)] in an itinerant magnet because the order parameter is not conserved. This behavior resembles the situation in dipolar magnets, where the peaks shift to $q = 0$ in the dipolar regime.^{29,30} Moreover, since the relaxation is not only controlled by exchange, even at T_c , the line shape at T_c differs from the asymptotic renormalization-group theory prediction. Therefore, the peak shape in constant- E scans is also different. The dependence of the line shape on the type of interaction is nicely exemplified for dipolar magnets.

The above interpretation is supported by neutron-scattering experiments in the metallic Heisenberg ferromagnet Pd₂MnSn above T_c by Koghi *et al.*,³³ where the anomalously large temperature dependence of the linewidth at small q has been explained by interactions of the localized moments with the conduction electrons. These effects become increasingly more important with increasing temperature because of the smearing of the Fermi surface. They are also expected to be important in Ni because the itinerant $3d$ electrons contribute directly to the formation of the magnetic moments.

V. SUMMARY

We have shown that the paramagnetic scattering cross section in Ni near T_c agrees qualitatively with the predictions of asymptotic renormalization-group theory for a Heisenberg ferromagnet. Minor discrepancies in line shapes occur already at T_c , however, far away from T_c and at small energy transfers they become more pronounced. A possible reason for the disagreement is the stronger damping of the spin fluctuations in Ni due to the conduction electrons. The scaling behavior of the constant- E scans for $1 \leq \hbar\omega \leq 45$ meV is an indication

that the dynamics of the spin fluctuations in the energy and momentum range investigated is of relaxational type. The asymptotic behavior of $S(q, \omega \rightarrow \infty)$ is proportional to $\omega^{-2.31}$ close to the value predicted by renormalization-group theory.

ACKNOWLEDGMENTS

Research at Brookhaven and Oak Ridge was supported by the Division of Material Sciences, U.S. Department of Energy under Contract Nos. DE-AC02-76CH00016 and DE-AC05-84OR21400, respectively.

*Formerly at Brookhaven National Laboratory, Upton, NY 11973.

¹T. Moriya, *Spin Fluctuations in Itinerant Electron Magnetism* (Springer, Berlin, 1985).

²H. A. Mook and D. McK. Paul, *Phys. Rev. Lett.* **54**, 227 (1985).

³D. McK. Paul, H. A. Mook, P. W. Mitchell, and S. M. Hayden, *J. Phys. (Paris) Colloq.* **49**, C8-59 (1988).

⁴J. F. Cooke, J. A. Blackman, and T. Morgan, *Phys. Rev. Lett.* **54**, 718 (1985).

⁵H. A. Mook, J. W. Lynn, and R. M. Nicklow, *Phys. Rev. Lett.* **30**, 556 (1973); J. W. Lynn and H. A. Mook, *Phys. Rev. B* **23**, 198 (1981).

⁶Y. J. Uemura, G. Shirane, O. Steinsvoll, and J. P. Wicksted, *Phys. Rev. Lett.* **51**, 2322 (1983).

⁷P. Böni and G. Shirane, *J. Appl. Phys.* **57**, 3012 (1985).

⁸P. Résibois and C. Piette, *Phys. Rev. Lett.* **24**, 514 (1970); C. Joukoff-Piette and P. Résibois, *Phys. Lett.* **42A**, 531 (1973).

⁹J. P. Wicksted, P. Böni, and G. Shirane, *Phys. Rev. B* **30**, 3655 (1984).

¹⁰R. Folk and H. Iro, *Phys. Rev. B* **32**, 1880 (1985).

¹¹V. Dohm, *Solid State Commun.* **20**, 657 (1976).

¹²K. Bhattacharjee and R. A. Ferrell, *Phys. Rev. B* **24**, 6480 (1981).

¹³P. Böni, M. E. Chen, and G. Shirane, *Phys. Rev. B* **35**, 8449 (1987).

¹⁴P. Böni, G. Shirane, H. G. Bohn, and W. Zinn, *J. Appl. Phys.* **63**, 3089 (1988).

¹⁵R. Folk and H. Iro, *Phys. Rev. B* **34**, 6571 (1986).

¹⁶H. Iro, *Z. Phys. B* **68**, 485 (1987).

¹⁷H. Iro, *J. Magn. Magn. Mater.* **73**, 175 (1988).

¹⁸J. Kötzler, *Phys. Rev. B* **38**, 12 027 (1988).

¹⁹P. Böni, G. Shirane, J. L. Martínez, and H. A. Mook, *Physica B* **180&181**, 219 (1992).

²⁰V. J. Minkiewicz, M. F. Collins, R. Nathans, and G. Shirane, *Phys. Rev.* **182**, 624 (1969).

²¹J. Skalyo, Jr. and N. A. Lurie, *Nucl. Instrum. Methods.* **112**, 571 (1973).

²²R. Anders and K. Stierstadt, *Solid State Commun.* **39**, 185 (1981).

²³P. Böni, J. L. Martínez, and J. M. Tranquada, *Phys. Rev. B* **43**, 575 (1991).

²⁴G. Shirane, P. Böni, and J. L. Martínez, *Phys. Rev. B* **36**, 881 (1987).

²⁵J. Als-Nielsen, O. W. Dietrich, and L. Passell, *Phys. Rev. B* **14**, 4908 (1976).

²⁶J. W. Lynn, *Phys. Rev. Lett.* **52**, 775 (1984).

²⁷Lee Chow and David Fisher, *Phys. Rev. B* **37**, 5848 (1988).

²⁸F. Mezei, B. Farago, S. M. Hayden, and W. G. Stirling, *Physica B* **156&157**, 226 (1989).

²⁹E. Frey and F. Schwabl, *Phys. Lett. A* **123**, 49 (1987); E. Frey, F. Schwabl, and S. Thoma, *ibid.* **129**, 343 (1988); *Phys. Rev. B* **40**, 7199 (1989).

³⁰C. Aberger and R. Folk, *Phys. Rev. B* **38**, 6693 (1988); **38**, 7207 (1988).

³¹H. A. Mook, *Phys. Rev. Lett.* **46**, 508 (1981).

³²P. Böni and G. Shirane, *Phys. Rev. B* **33**, 3012 (1986).

³³M. Koghi, Y. Endoh, Y. Ishikawa, H. Yoshizawa, and G. Shirane, *Phys. Rev. B* **34**, 1762 (1986).